*Срочно прочитать, исправить ошибки и позвонить
в редакцию (499) 132 66 66, (499) 135 13 11.*

Diagnostics of optical anisotropy changes in biological tissues using Müller matrix

Yu.A. Ushenko, Yu.Ya. Tomka, A.V. Dubolazov, O.Yu. Telen'ga

Abstract. We study the efficiency of Müller matrix diagnostics of birefringence in biological tissue layers with different optical thickness by measuring a set of third- and fourth-order statistical moments, characterising the coordinate distributions of the matrix element Z_{44} at different points of the histological section.

1. Introduction

During the last 10 years the variety of optical methods for structure diagnostics of organic phase-inhomogeneous objects has been replenished with a new method, namely, the laser polarimetry [1 – 22]. Laser polarimetry diagnostics provides information on optical anisotropy [2 – 5, 18, 19, 23] of biological tissues (BTs) in the form of coordinate distributions of the Müller matrix element, or Müller matrix images (MMI), of BTs. To analyse such polarimetric information a model approach has been developed [1, 2, 7, 8, 21, 24], in which the following assumptions are used:

(i) the whole variety of human BTs is divided into four basic types, namely, the connective, muscular, epithelial and neural tissues;

(ii) morphologically, a BT of any type has a two-component amorphous-crystal structure;

(iii) the crystal component, or extracellular matrix, is formed by a network of protein (collagen, myosin, elastin, etc.) fibrils;

(iv) protein fibrils possess the properties of uniaxial birefringent crystals, whose polarisation properties are described by the Müller matrix [1, 7, 8, 26]

$$\{Z\} = \begin{Vmatrix} 1 & 0 & 0 & 0 \\ 0 & z_{22} & z_{23} & z_{24} \\ 0 & z_{32} & z_{33} & z_{34} \\ 0 & z_{42} & z_{43} & z_{44} \end{Vmatrix}, \tag{1}$$

where

Yu.A. Ushenko, Yu.Ya. Tomka, A.V. Dubolazov, O.Yu. Telen'ga Yuriy Fedkovych Chernivtsi National University, ul. Kotsubinsky 2, 58012 Chernivtsi, Ukraine, e-mail: yuriyu@gmail.com

$$z_{ik} = \begin{cases} z_{22} = \cos^2 2\rho + \sin^2 2\rho \cos \delta, \\ z_{23,32} = \cos 2\rho \sin 2\rho (1 - \cos \delta), \\ z_{33} = \sin^2 2\rho + \cos^2 2\rho \cos \delta, \\ z_{34,43} = \pm \cos 2\rho \sin \delta, \\ z_{24,42} = \pm \sin 2\rho \sin \delta, \\ z_{44} = \cos \delta; \end{cases} \tag{2}$$

ρ is the optical axis direction, determined by the stacking direction of protein fibrils with the geometrical cross section size d and the birefringence index Δn; $\delta = (2\pi/\lambda)\Delta nd$ is the phase shift, arising between the orthogonal components of the laser field having the wave length λ.

This model was used to find and justify the mutual relation between the set of the first-to-fourth-order statistical moments, characterising the orientation-phase structure (distributions of the optical axes directions and phase shifts) of the extracellular matrix in optically thin (the attenuation coefficient $\tau \leqslant 0.1$) BT layers, and the statistical moments, describing the coordinate distribution of the Müller matrix elements [1, 21, 27]. It is established [12] that the third- and fourth-order statistical moments of the distributions of the matrix elements z_{24}, z_{34}, z_{44} of the extracellular BT matrix are most sensitive to the changes in the optical anisotropy of the networks of protein crystals. On this base the optical criteria for early diagnostics of muscular dystrophy, precancerous states of connective tissue, collagen disease, etc., were formulated [12, 19, 22, 26, 28]. However, such methods do not account for the spatial inhomogeneity of the networks of protein crystals and for the multiplicity of light scattering within the BT thickness. That is why it is urgent to study not only the values of the statistical first to fourth-order moments, but also their distributions, characterising 2D elements of the Müller matrix within the whole BT layer.

The present paper is devoted to the study of possibilities of laser diagnostics of optical anisotropy in BTs having different optical thicknesses and physiological condition on the basis of the statistical approach to the analysis of the coordinate distributions of the 2D elements of the Müller matrix.

2. The scheme and the technique of measuring the coordinate distributions of Müller matrix elements in biological tissues

Figure 1 shows the traditional optical scheme of a polarimeter for measuring the coordinate distributions of the Müller matrix elements in the BT [1, 7, 8, 21].

The illumination of histological sections of the BT was accomplished using a parallel radiation beam with the
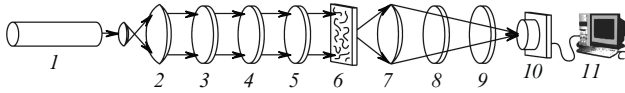
Figure 1. Optical scheme of the polarimeter: (*1*) He–Ne laser; (*2*) collimator; (*3*) steady-state quarter-wave plate; (*4*) polariser; (*5*, *8*) mechanically movable quarter-wave plates; (*6*) studied object; (*7*) microscope objective; (*9*) analyser; (*10*) CCD-camera; (*11*) personal computer.

radius $r = 1$ mm from a 0.6328-μm, 5.0-W He–Ne laser. The polarisation light source consists of the quarter-wave plates (*3*, *5*) and the polariser (*4*). By means of the microscope objective (*7*) the polarisation images of the BT were projected onto the plane of the light-sensitive area ($m \times n = 800 \times 600$ pixels) of the CCD-camera (*10*). The BT image analysis was implemented using the polariser (*9*) and the quarter-wave plate (*8*). The technique of measuring the Müller matrix elements is described in detail in the monograph by Gerrard [6]. In the present paper we restrict ourselves with its brief statement.

The elements of the BT Müller matrix are determined in the following way:

$$
\begin{bmatrix} S_1 \\ S_2 \\ S_3 \\ S_4 \end{bmatrix} = \begin{bmatrix} z_{11} & z_{12} & z_{13} & z_{14} \\ z_{21} & z_{22} & z_{23} & z_{24} \\ z_{31} & z_{32} & z_{33} & z_{34} \\ z_{41} & z_{42} & z_{43} & z_{44} \end{bmatrix} \begin{bmatrix} S_{01} \\ S_{02} \\ S_{03} \\ S_{04} \end{bmatrix}, \tag{3}
$$

where S_0, S are the Stokes vectors of the probe and object laser beams.

The elements z_{ik} of the Müller matrix for each pixel of the digital camera were determined in correspondence with the following algorithm:

(i) The intensities I_0, I_{90}, I_{45}, I_{-45}, $I_{\oplus}$ (right-hand circular polarisation) and $I_{\otimes}$ (left-hand circular polarisation) were measured sequentially followed by determination of the Stokes parameters of the object beam:

$$
\begin{aligned}
S_1 &= I_0 + I_{90}, \\
S_2 &= I_0 - I_{90}, \\
S_3 &= I_{45} - I_{-45}, \\
S_4 &= I_{\otimes} - I_{\oplus}.
\end{aligned} \tag{4}
$$

(ii) The histological section of the biological tissue was illuminated with laser beams in the four basic polarisation states ($0°$, 90, $+45°$, $\otimes$) and relations (4) were used to determine the Stokes parameters of the object beam:

$$
\begin{aligned}
S_1^0 &= z_{11} + z_{12}, & S_1^{90} &= z_{11} - z_{12}, \\
S_1^{45} &= z_{11} + z_{13}, & S_1^{\otimes} &= z_{11} + z_{14}, \\
S_2^0 &= z_{21} + z_{22}, & S_2^{90} &= z_{21} - z_{22}, \\
S_2^{45} &= z_{21} + z_{23}, & S_2^{\otimes} &= z_{21} + z_{24}, \\
S_3^0 &= z_{31} + z_{32}, & S_3^{90} &= z_{31} - z_{32}, \\
S_3^{45} &= z_{31} + z_{33}, & S_3^{\otimes} &= z_{31} + z_{34}, \\
S_4^0 &= z_{41} + z_{42}, & S_4^{90} &= z_{41} - z_{42}, \\
S_4^{45} &= z_{41} + z_{43}, & S_4^{\otimes} &= z_{41} + z_{44}.
\end{aligned} \tag{5}
$$

From Eqns (5) the elements of the Müller matrix of the BT layer were found

$$
\begin{aligned}
z_{11} &= 0.5(S_1^0 + S_1^{90}), & z_{21} &= 0.5(S_2^0 + S_2^{90}), \\
z_{31} &= 0.5(S_3^0 + S_3^{90}), & z_{41} &= 0.5(S_4^0 + S_4^{90}), \\
z_{12} &= 0.5(S_1^0 - S_1^{90}), & z_{22} &= 0.5(S_2^0 - S_2^{90}), \\
z_{32} &= 0.5(S_3^0 - S_3^{90}), & z_{42} &= 0.5(S_4^0 - S_4^{90}), \\
z_{13} &= S_1^{45} - z_{11}, & z_{23} &= S_2^{45} - z_{21}, \\
z_{33} &= S_3^{45} - z_{31}, & z_{43} &= S_4^{45} - z_{41}, \\
z_{14} &= S_1^{\otimes} - z_{11}, & z_{24} &= S_2^{\otimes} - z_{21}, \\
z_{34} &= S_3^{\otimes} - z_{31}, & z_{44} &= S_4^{\otimes} - z_{41},
\end{aligned} \tag{6}
$$

after which the set of their reduced values $z_{ik} = z_{ik}/z_{11}$ was determined.

Within the limits of the laser beam cross section having the radius $r = 1$ mm the MMI arrays of the values of the elements Z_{ik} ($m \times n$) of the Müller matrix were determined ($m \times n = 800 \times 600$ pixels). Then, the plane of the BT histological section (nearly 10×20 mm) was subjected to line-by-line laser beam scanning with the linear displacement step of $\Delta r = 2$ mm. Within each of the 50 regions ($j = 1, 2, \ldots, 50$) of the illuminated BT layer the local arrays $Z_{ik}^{(j)}$ were determined following the algorithm (6):

$$
Z_{ik}^{(j)} = \begin{pmatrix} Z_{ik}^{11} & \ldots & Z_{ik}^{1m} \\ \ldots & \ldots & \ldots \\ Z_{ik}^{n1} & \ldots & Z_{ik}^{nm} \end{pmatrix}_j. \tag{7}
$$

For each MMI element $Z_{ik}^{(j)}$ the statistical moments of the third ($M_j^{(s=3)}$-skewness) and fourth ($M_j^{(s=4)}$-kurtosis) orders were calculated using the following relations:

$$
M_j^{(s=3)} = \frac{1}{\left(M^{(s=2)}\right)^3} \frac{1}{N} \sum_{i=1}^{N} \left(Z_{ik}^{(j)}\right)^3, \tag{8}
$$

$$
M_j^{(s=4)} = \frac{1}{\left(M^{(s=2)}\right)^4} \frac{1}{N} \sum_{i=1}^{N} \left(Z_{ik}^{(j)}\right)^4. \tag{9}
$$

Here, $M_j^{(s=2)}$ is the variance of $Z_{ik}^{(j)}$.

Based on Eqns (8) and (9), the histograms $N(M_j^{(s=3,4)})$ were determined for the set of higher-order statistical moments, characterising 2D distributions of the matrix elements $Z_{ik}^{(j)}$ within all 50 illuminated regions of the histological sections of the studied BTs.

3. Study of distributions of the MMI skewness and kurtosis for the element Z_{44} in histological sections of biological tissues

As the objects of study we have chosen three groups of histological sections of the basic BT types of a rat:

(i) group A – the connective tissue (skin dermis);
(ii) group B – the muscular tissue (skeletal muscle tissue);
(iii) group C – the epithelial tissue.

This choice of the objects allows the comparative study of the efficiency of Müller matrix method of the birefringence change diagnostics both within one group of samples and for different types of BTs. Moreover, the study of the rat BTs allows the realisation of direct experimental formation of septic inflammation and the implementation of Müller matrix monitoring of its optical manifestations

under the conditions of the laser radiation scattering of different multiplicity. With this aim the optically thin (the attenuation coefficient $\tau \leqslant 0.1$) and optically thick ($\tau \geqslant 0.1$) histological sections of the studied BT samples were chosen.

In this paper we restrict ourselves to the analysis of histograms of the third and fourth-order statistical moments, which characterise the 2D distributions of the matrix element Z_{44}. The choice of the matrix element Z_{44} is determined by the fact that its value [$z_{44} \propto (2\pi/\lambda)\Delta nd$, see Eqns (2)] directly characterises the optical birefringence Δn of the protein fibrils of the extracellular matrix in the BT layer.

Figures 2–4 show the MMI coordinate distributions of the matrix element Z_{44} for histological sections of connective (Fig. 2), muscular (Fig. 3) and epithelial (Fig. 4) tissue of a rat.

One can see from the obtained experimental data that the MMI of the matrix element Z_{44} is coordinate inhomoge-
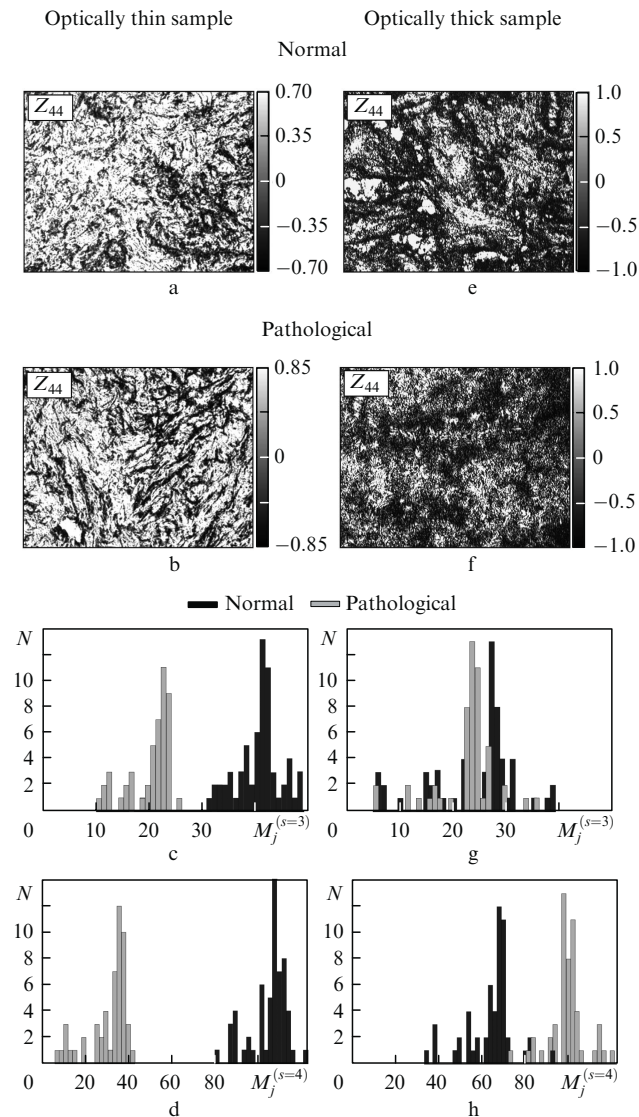

Figure 3. Coordinate distributions of the element Z_{44} in histological sections of optically thin (a, b) and optically thick (e, f) layers of healthy (a, e) and inflamed (b, f) rat skeletal muscle tissue. The fragments (c) and (d) correspond to histograms $N(M_j^{(s=3,4)})$ of higher-order statistical moments $M_j^{(s=3,4)}$ of optically thin, and (g) and (h) of optically thick layers.

Figure 2. Coordinate distributions of the element Z_{44} in histological sections of optically thin (a, b) and optically thick (e, f) layers of healthy (a, e) and inflamed (b, f) rat skin dermis. The fragments (c) and (d) correspond to histograms $N(M_j^{(s=3,4)})$ of higher-order statistical moments $M_j^{(s=3,4)}$ of optically thin, and (g) and (h) of optically thick layers.
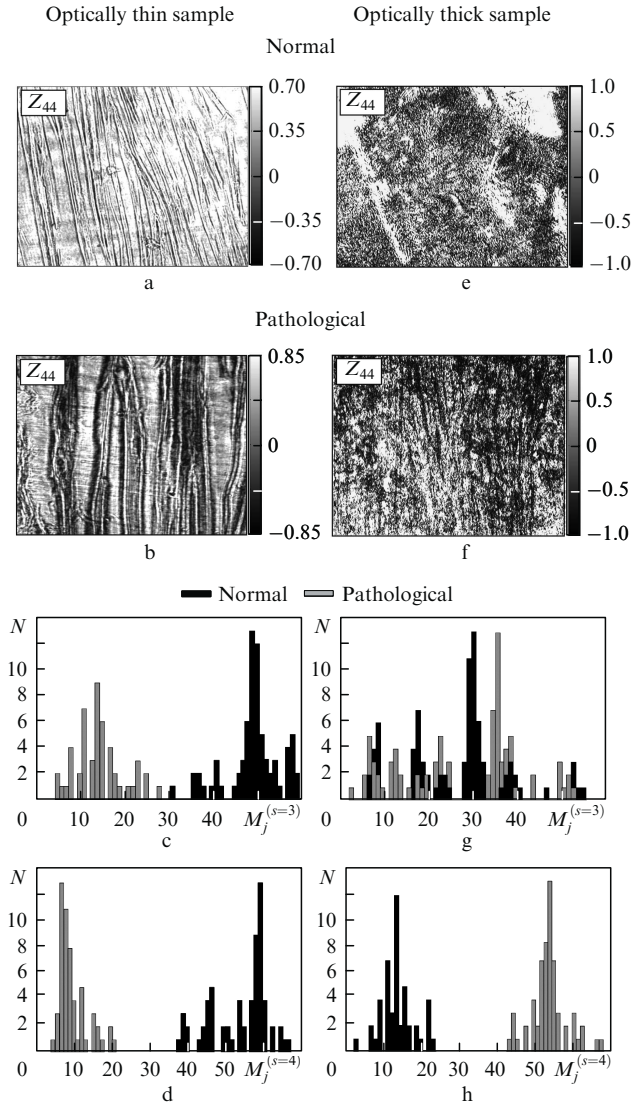
neous for all types of BTs. For optically thin histological sections of the samples of healthy connective, muscular and epithelial tissues, the typical range of variation of the matrix element Z_{44} is smaller (from -0.7 to 0.7) than that for the samples of inflamed tissues (from -0.85 to 0.85). This property character of the MMI structure of the matrix element Z_{44} can be attributed to the fact that when a laser wave propagates through a network of optically anisotropic protein (collagen, myosin, elastin) fibrils, a broad spectrum of phase shift values δ_k is formed, proportional to their geometrical sizes d_k in the plane of the histological section of the BT:

$$\delta_k \propto \frac{2\pi\Delta n}{\lambda} d_k. \tag{10}$$

The inflammation process in the BT is accompanied with the growth of birefringence Δn due to formation of protein fibril edema. From the optical point of view, this physio-

Optically thin sample   Optically thick sample

Normal

a

e

Pathological

b

f

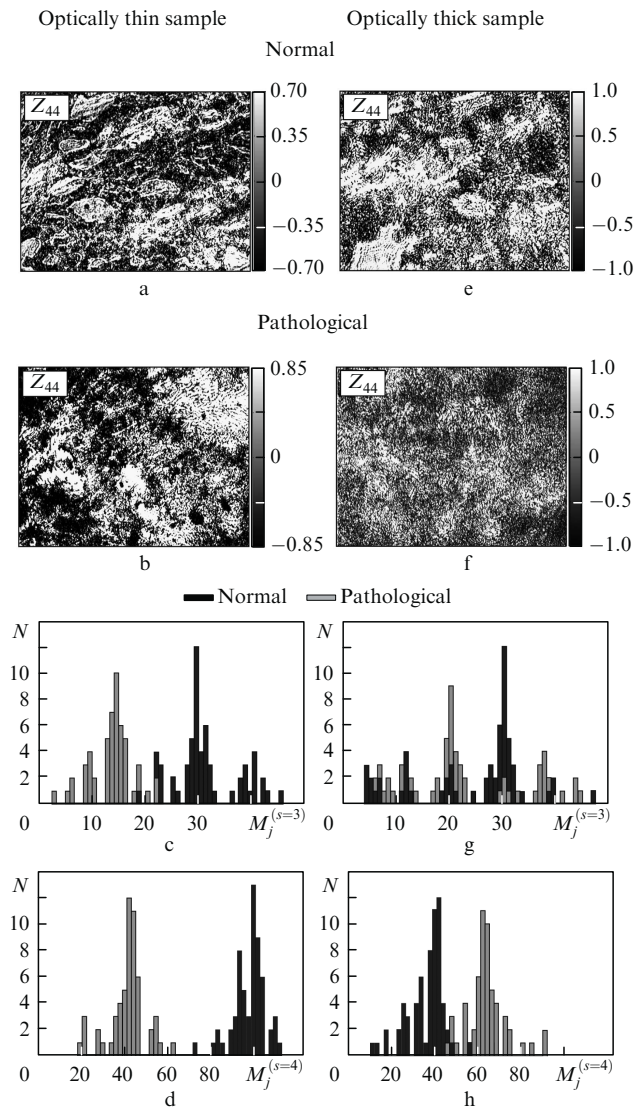**Normal** **Pathological**

c

g

d

h

Figure 4. Coordinate distributions of the element Z_{44} in histological sections of optically thin (a, b) and optically thick (e, f) layers of healthy (a, e) and inflamed (b, f) rat epithelial tissue. The fragments (c) and (d) correspond to histograms $N(M^{(s=3,4)})$ of higher-order statistical moments $M_j^{(s=3,4)}$ of optically thin, and (g) and (h) of optically thick layers.

logical process leads to the increase in the range of variation in phase shifts δ_k and to the associated growth of fluctuations of the matrix elements Z_{44} values (Figs 2–4).

The analysis of the histograms $N(M_j^{(s=3,4)})$ of the values $M_j^{(s=3,4)}$ of coordinate distributions of the matrix element $Z_{44}^{(j)}$ in optically thin layers of BT has revealed the following:

(i) the ranges of variation of the values of skewness $M_j^{(s=3)}$ and the kurtosis $M_j^{(s=4)}$, measured at different points of the layers of healthy and inflamed biological tissues of a rat, do not coincide;

(ii) the extreme values $M_j^{(s=3)}$ and $M_j^{(s=4)}$ of the corresponding histograms $N(M_j^{(s=3,4)})$ for samples of healthy tissues are greater than the analogous values of the third- and fourth-order statistical moments for inflamed tissues, namely, 2–3 times greater for connective tissue, 4–6 times greater for muscular tissue, and 1.5–2 times greater for epithelial tissue.

Thus, for unambiguous differentiation of the physiological condition of optically thin layers of BTs it is

sufficient to measure the coordinate $(m \times n)$ distribution of the matrix element Z_{44} in one domain (with the area πr^2), irradiated with a laser beam, and to calculate the values $M_j^{(s=3)}$ and $M_j^{(s=4)}$.

For optically thick layers of healthy and inflamed tissues of all groups (Figs 2–4) we deal with the same region of variation of the values of the matrix elements Z_{44}. This fact may be associated with the multiplicity of light scattering inside the bulk BT. As a result of each local (ith) act of interaction between the laser radiation and a separate fibril, the random phase shift $\delta^{(i)}$ is formed, whose value experiences 'multiplication' ($\delta^* = \sum_{i=1}^k \delta_i$) in the course of further propagation in the bulk BT attaining equiprobable random values from 0 to $2k\pi$ ($k = 1, 2, 3, \ldots$).

The analysis of the histograms $N(M_j^{(s=3,4)})$ of the set of values of statistical moments $M_j^{(s=3)}$ and $M_j^{(s=4)}$, characterising the distribution of $Z_{44}^{(j)}$ for optically thick layers of rat tissues, has shown that

(i) the ranges of the skewness $M_j^{(s=3)}$ variation for the distributions of $Z_{44}^{(j)}$, measured over the whole plane of the healthy and inflamed BT samples, practically coincide and cannot serve as an objective test for differentiation of their optical properties;

(ii) the histograms $N(M_j^{(s=4)})$ of the kurtosis $M_j^{(s=4)}$ values for the distributions of $Z_{44}^{(j)}$ are individual for each BT type and its physiological condition;

(iii) the difference of kurtosis $M_j^{(s=4)}$ values for the distributions of $Z_{44}^{(j)}$ between the samples of healthy and inflamed tissue is from 1.25 (skin dermis) to 4 (muscular tissue) times.

Hence, the objective base to implement the Müller matrix differentiation in optically thick BT layers at early stages of the change in their physiological condition is provided by measuring histograms of the kurtosis $N(M_j^{(s=4)})$ values, specifying the coordinate distribution of the matrix element $Z_{44}^{(j)}$.

4. Conclusions

It is established that to solve the problem of differentiation of BT physiological condition in optically thin samples it is sufficient to determine the values of the skewness $M^{(s=3)}$ and the kurtosis $M^{(s=4)}$, specifying the coordinate distribution of Z_{44} in an arbitrary area, probed with the laser beam.

For optically thick samples the most objective test is to find the extreme values of the fourth-order statistical moment, which specifies the histograms $N(M_j^{(s=4)})$ of the kurtosis local values of the coordinate distributions of the element $Z_{44}^{(j)}$ in different (jth) regions of the layers of BTs under diagnostics.

References

1. Ushenko A.G., Pishak V.P., in *Coherent-Domain Optical Methods: Biomedical Diagnostics, Environmental and Material Science* (Boston: Kluwer Acad. Publ., 2004) pp 67–93.
2. De Boer J.F., Milner T.E. *J. Biomed. Opt.*, **7**, 359 (2002).
3. De Boer J.F., Milner T.E., Nelson J.S., in *Trends in Optics and Photonics (TOPS): Advances in Optical Imaging and Photon Migration* (Washington, DC: OSA, 1998).
4. Everett M.J., Shoenenberger K., Colston B.W., Da Silva L.B. *Opt. Lett.*, **23**, 228 (1998).
5. Shuliang Jiao, Wurong Yu, George Stoica, Lihong V. Wang. *Opt. Lett.*, **28**, 1206 (2003).

6. Gerrard A., Burch J.M. *Introduction to Matrix Methods in Optics* (New York: Wiley, 1975).

7. Angelsky O.V., Ushenko A.G., Ushenko Yu.A., Pishak V., in *Optical Correlation Techniques and Applications* (Washington: Soc. Photo-Opt. Instrum. Eng., 2007) pp 213 – 266.

8. Angelsky O.V., Ushenko A.G., Ushenko Yu.A., Pishak V., Peresunko A., in *Handbook of Photonics for Biomedical Science* (New York: CRC Press, 2010) pp 21 – 67.

9. Ushenko Alexander G. *Opt. Eng.*, **34** (4), 1088 (1995).

10. Ushenko A.G., Ermolenko S.B., Burkovets D.N., Ushenko Yu.A. *Opt. Spektrosk.*, **87** (3), 470 (1999) [*Opt. Spectrosc.*, **87** (3), 434 (1999)].

11. Ushenko A.G. *Opt. Spektrosk.*, **89** (4), 651 (2000) [*Opt. Spectrosc.*, **89** (4), 597 (2000)].

12. Angel'skii O.V., Ushenko A.G., Ermolenko S.B., Burkovets D.N., Pishak V.P., Ushenko Yu.A., Pishak O.V. *Opt. Spektrosk*. **89** (5), 866 (2000) [*Opt. Spectrosc.*, **89** (5), 799 (2000)].

13. Angel'skii O.V., Ushenko A.G., Arkhelyuk A.D., Ermolenko S.B., Burkovets D.N., Ushenko Yu.A. *Opt. Spektrosk.*, **89** (6), 1050 (2000) [*Opt. Spectrosc.*, **89** (6), 973 (2000)].

14. Ushenko A.G. *Laser Phys.,* **10** (5), 1143 (2000).

15. Ushenko A.G., Ermolenko S.B., Burkovets D.N., Ushenko Yu.A. *J. Appl. Spectrosc.*, **67** (1), 65 (2000).

16. Angel'skii O.V. , Ushenko A.G., Arheluk A.D., Ermolenko S.B., Burkovets D.N., Ushenko Y.A. *J. Appl. Spectrosc.*, **67** (5), 919 (2000).

17. Ushenko A.G., Burkovets D.N., Ushenko Y.A. *Laser Phys.*, **11** (5), 624 (2001).

18. Angel'skii O.V., Ushenko A.G., Burkovets D.N., Ushenko Yu.A. *Opt. Spektrosk.*, **90** (3), ??? (2001) [*Opt. Spectrosc.*, **90** (3), 458 (2001)].

19. Ushenko A.G. *Opt. Spektrosk.*, **91** (2), ??? (2001) [*Opt. Spectrosc.*, **91** (2), 313 (2001)].

20. Ushenko A.G. *Opt. Spektrosk.*, **91** (6), ??? (2001) [*Opt. Spectrosc.* **91** (6), 932 (2001)].

21. Angelsky O.V., Ushenko A.G., Ushenko Yu.A. *J. Holography and Speckle*, **2** (2), 72 (2002).

22. Ushenko A.G., Burkovets D.N., Ushenko Yu.A. *Opt. Spektrosk.*, 93 (3), ??? (2002) [*Opt. Spectrosc.* **93** (3), 449 (2002)].

23. Angelsky Oleg V., Ushenko Alexander G., Burkovets Dimitry N., Ushenko Yuriy A. *Opt. Applicata*, **32** (4), 591 (2002).

24. Angelsky Oleg V., Demianovsky G.V., Ushenko A.G., Burkovets D.N., Ushenko Yu.A. *J. Biomed. Opt.*, **9**, 679 (2004).

25. Angelsky Oleg V., Ushenko Alexander G., Burkovets Dimitry N., Ushenko Yuriy A. *J. Biomed. Opt.*, **10**, 014010 (2005).

26. Angelsky O.V., Ushenko A.G., Ushenko Ye.G. *J. Holography and Speckle*, **2** (1), 26 (2005).

27. Angelsky Oleg V., Ushenko Alexander G., Burkovets Dimitry N., et al. *J. Phys. D: Appl. Phys.*, **38** (23), 4227 (2005).

28. Angelsky O.V., Ushenko A.G., Ushenko Ye.G. *Phys. Med. Biol.*, **50**, 4811 (2005).